

Penetration Mechanism of Partial Penetration Electron Beam Welding

A new technique utilizing a pinhole X-ray camera can record secondary X-radiation given off at the point of impact to reveal the characteristics of beam-metal interaction and the spiking phenomenon

BY C. M. WEBER, E. R. FUNK AND R. C. McMASTER

ABSTRACT. A new technique has been developed to observe the penetration mechanism of partial penetration electron beam welding. This technique involves the use of a pinhole X-ray movie camera to record the secondary X-radiation given off at the point of impact of the electron beam and the metal. The characteristics of beam-metal interaction are in part revealed. An explanation of how spiking occurs in partial penetration welds is proposed.

Introduction

In electron beam welding, a well defined stream of high energy electrons is used to bombard the work material to produce a fusion joint. The energy densities developed in electron beam welding are considerably greater than those of the more conventional welding processes. As a consequence, electron beam welding possesses some unusual characteristics. These include a very narrow heat affected zone, rapid welding speeds and very deep penetration.

Little is known, however, about the

actual mechanism that occurs during electron beam welding.^{1,2} For this reason, a program was initiated in which an X-ray pinhole movie camera was used to observe the events occurring in the cavity. As a result, the penetration mechanism is illuminated. Variations in the penetration mechanism are seen to be responsible for the phenomenon of spiking and some other defects.

Experimental Procedure

An X-ray pinhole movie camera was constructed to provide a continuous recording of the events occurring in the cavity. A schematic diagram is given in Fig. 1.

A direct correlation can be made between the location of the exposure on the film and the location of the source of the X-radiation. This technique reveals the location in the weld cavity where electrons from the electron beam are colliding with metallic atoms in the weld cavity, since X-radiation is emitted from such collisions.

The pinhole used with this camera is cone-shaped and made in $1/8$ in.

lead. A cone-shaped pinhole is necessary since the length of the pinhole ($1/8$ in.) is large compared with the other dimensions. This construction allows for the passage of X-rays that are not aligned with the axis of the pinhole. For example, a cylindrically shaped pinhole would attenuate those X-rays that were not aligned with the axis of the pinhole.

This pinhole is mounted to the face plate of the camera which is also of $1/8$ in. lead. Figure 2 is a picture of the pinhole camera used for this experiment. It contains, in addition to the spools for the X-ray movie film and the driving mechanism, a timing device. This device consists of a small neon bulb wrapped in electrical tape with a hypodermic needle directing the light to the film. With an audio oscillator and an amplifier, timing dots are placed on the film to record the film speed.

The film used during this experiment is 35 mm \times 25 feet Kodak "No-Screen." This is a high speed X-ray movie film not requiring intensifying screens.

The electron beam welding machine is a Hamilton-Standard Model

C. M. WEBER is Senior Welding Engineer, Research Center, Babcock & Wilcox, Inc., Alliance, Ohio. E. R. FUNK is Associate Professor, Welding Engineering Department and R. C. McMASTER is Regents Professor, both of The Ohio State University, Columbus, Ohio.

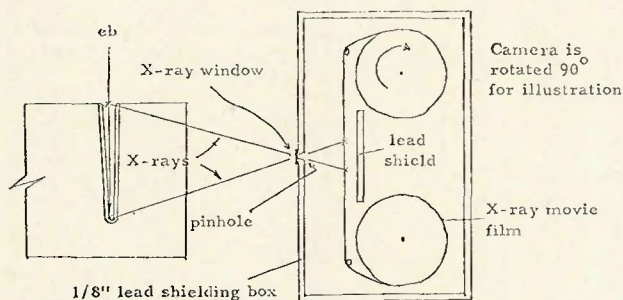


Fig. 1—Sketch shows details of pinhole camera technique

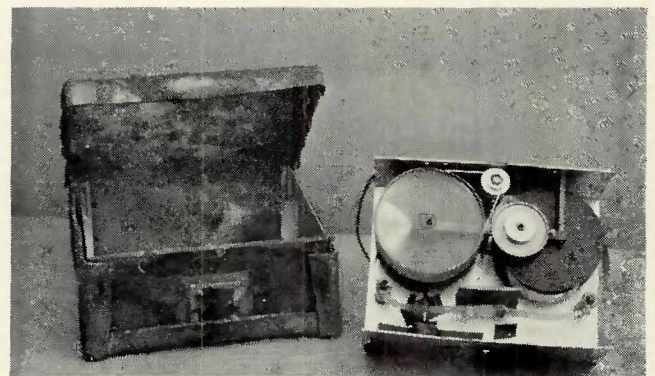


Fig. 2—Photograph of pinhole camera reveals working mechanism and lead shielding box with pinhole used for this experiment

#W1-0 rated at 3 KW. It should be mentioned that a high voltage machine is necessary for this experiment since the generated X-rays must have sufficient energy so as not to be attenuated in the material.

An additional recording device was also used in conjunction with the X-ray camera. This device is a copper grid located 1 in. above the work for the purpose of monitoring the voltage that develops in this region during welding.

For comparison with the X-ray exposure and the grid voltage trace, the EB welds were sectioned longitudinally by grinding and polishing to reveal maximum penetration. Because of the spike-like nature of the EB fusion zone, extreme care must be exercised to assure that the longitudinal section is at the point of maximum penetration (weld centerline). Photomicrographs of these sections are then made for comparison with the X-ray exposure.

Another technique was also used for correlation with the X-ray exposures. Difficulties in revealing the maximum penetration by the grinding and polishing method can be removed by welding on a butt joint. By surface grinding the faces of the butt joint and welding along the joint, the subsequent cracking open of that joint will reveal the maximum penetration.

Unfortunately, the welding conditions were crudely monitored. A digital voltmeter was used to measure the accelerating potential. Beam current measurements were made with the meter supplied with the welding machine. The focal area of the beam was held constant to a surface focus. The dimensions of this area were established by observation through the supplied telescope system. The average welding speed was computed by measuring the length of the weld from the longitudinal macrograph and dividing this distance by the total welding time. Weld time is obtained by counting the timing dots on the X-ray exposure.

The accelerating voltage was varied between 130 and 150KV, while the beam current was varied between 5 ma and 10 ma. These two parameters were not varied widely since a large number of energetic X-rays is desired to assure an exposure on the X-ray film in the pinhole camera. The focal area was intended to remain constant while welding speed variations occurred between 0 ipm and 24 ipm. The materials used were 1100 aluminum, 6061 aluminum, 1020 steel, type 410 stainless steel and ETP copper. Welding conditions for various attempts are given in Table 1.

Table 1—Welding Conditions

Run number	Material	Voltage Kv	Beam current milli-amperes	Focal area mils	Welding speed cm/sec
12	1020 steel	150	5	6 × 4	0.00
13	1020 steel	150	5	6 × 4	0.62
14	1020 steel	150	5	6 × 4	0.00
17	6061 aluminum	150	10	6 × 4	0.00
18	6061 aluminum	150	10	6 × 4	—
19	6061 aluminum	150	10	6 × 4	0.99
20	6061 aluminum	150	10	6 × 4	—
22	6061 aluminum	130	7	6 × 4	0.53
23	6061 aluminum	130	7	6 × 4	0.00
24	6061 aluminum	130	7	6 × 4	0.84
25	6061 aluminum	150	10	6 × 4	0.52
26	6061 aluminum	150	10	6 × 4	0.00
27	1100 aluminum	150	10	6 × 4	—
29	6061 aluminum	150	10	6 × 4	0.00
30	1100 aluminum	150	10	6 × 4	—
31	1100 aluminum	130	7	6 × 4	0.00
32	1100 aluminum	130	7	6 × 4	0.00
33	1100 aluminum	130	7	6 × 4	1.01
35	ETP copper	150	9.5	6 × 4	0.00
36	ETP copper	150	9.5	6 × 4	0.00
37	ETP copper	150	10	6 × 4	1.01
39*	1020 steel	150	10	6 × 4	0.93
40*	6061 aluminum	150	10	6 × 4	0.93
41*	410 stainless	150	10	6 × 4	0.93

* Welds made on butt joints

Table 2—Comparison of Penetrations Obtained From X-Ray Exposures With Sectioned Welds

Run number	Maximum initial ^a penetration from macrograph	Maximum initial ^b penetration for x-ray exposure	Percent difference
12	0.358 cm ^c	0.396 cm ^c	4.8 %
13	0.327	0.402	18.6
14	0.288	0.500	42.4
17	1.300	<1.23	—
18	0.590	0.590	1.7
19	0.384	0.540	29.0
20	0.362	0.384	5.7
22	0.178	0.165	7.3
23	0.677	0.829	18.4
24	0.116	0.124	6.5
39 ^d	0.786	0.770	2.03π
40 ^d	0.834	0.852	2.16π
41 ^d	0.950	0.912	4.0 π

^a Maximum penetration occurring at weld start

^b Maximum penetration occurring within 0.1 sec from initiation of beam. It is assumed that within this time span at these welding speeds, specimen will not have moved significantly. Thus, penetration should correlate with initial penetration from macrograph

^c For cases where $V_w = 0$, value given is maximum penetration for duration of weld

^d Welds made on butt joints and cracked open to reveal penetrations

Results

To assure that the X-ray exposures of the weld are directly related to the actual penetration, a comparison is made between the penetration determined from the film and the actual penetration. Since the X-ray exposure is a continuous monitor of the penetration, the initial penetration was chosen as the point for comparison. For definition purposes, the initial penetration used for comparison is the maximum penetration seen on the film during the first 0.10 sec of the weld. It

is this value of the penetration that is used for correlation with the actual initial penetration (actual penetration at the start of the weld). For those cases where the welding speed is zero, the maximum penetration on the film occurring during the entire run is used for comparison. Table 2 summarizes the results of these comparisons.

The penetrations for Run No. 12 to No. 24 were revealed by grinding to the weld centerline (i.e., a longitudinal section). Figures 3 and 4 illustrate how penetration is revealed by this technique.

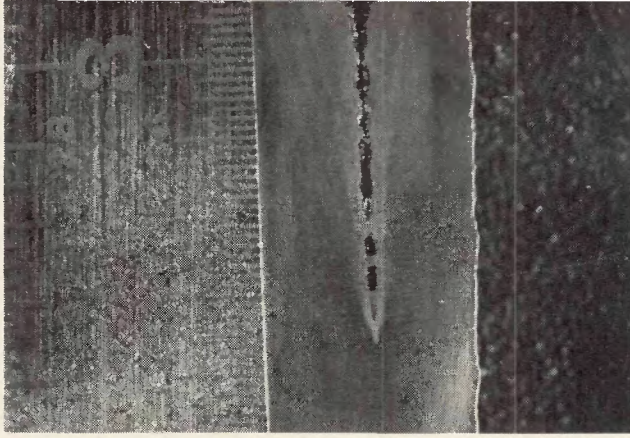


Fig. 3—Macrograph of sectioned weld No. 17; material: 6061 aluminum; welding conditions: $V = 150\text{KV}$, $i = 10\text{ ma}$; $v_w = 0\text{ ipm}$; etch: Kalling's reagent; Mag: 3.69X

Runs 39 to 41 were made on butt joints. Actual penetration for these runs was revealed by cracking the joint open. Figure 7a illustrates penetration revealed by joint cracking.

The primary value of the X-ray exposures is the study that can be made of the penetration mechanism. Three typical prints of exposures are given in Figures 5 to 7. These prints illustrate the mechanism and are typical of all the exposures. Figure 7 is a three-way correlation, in time, between the X-ray exposure, grid voltage trace and a macrograph of the cracked joint.

Discussion

The location of exposed regions on the X-ray film in the pinhole camera can be directly related to the location of EB electron collisions in the weld cavity. The magnification of the image is known from the geometry of the exposure. Thus, one can determine the location in the cavity where material intercepts the electron beam.

To check that the pinhole camera is "seeing" correctly, the penetration of welds No. 12 to No. 24 were measured by making a longitudinal section of the weld. The penetration was also determined from the X-ray exposure. A comparison of these two values (given in Table 2) for runs 12 to 24 shows lack of agreement.

Since this inconsistency seems theoretically impossible, it was assumed that the value of the penetration obtained by longitudinally sectioning to the weld centerline was incorrect. The spike-like nature of the fusion zone for an electron beam weld requires precision in this grinding operation. Slightly overshooting or undershooting the point of maximum penetration would result in an apparent penetration that could be drastically different from the actual maximum penetration (which the X-ray film is recording).

To demonstrate that the inconsistency is a result of inaccurate grinding

to the point of maximum penetration rather than an error in the camera system, three butt joints with surface ground faces were welded with the beam aligned with the joint. Subsequent cracking of these joints will reveal the maximum penetration. Now the comparison between actual penetration and that "seen" by the film can be made. Excellent agreement is obtained as can be seen for runs 39, 40 and 41 in Table 2. Thus, the disagreement noticed for runs 12 to 24 is attributed to inadequate grinding at the welded centerline which did not expose the maximum penetration. As expected, the film is accurately recording information.

From the data for runs 39, 40 and 41, one can get an appreciation of the dimension of the liquid layer surrounding the cavity at the base. The electron beam will impinge on the liquid surface at the base of the cavity. This is the penetration recorded by the film. By cracking open the butt joint and measuring the penetration, one is actually measuring the height of the cavity plus the thickness of the liquid layer at the cavity base plus the thickness of a region that is later melted by thermal conduction as the beam moves on. The comparison of these two measurements will give some idea as to the thickness of this layer. It is seen that the thickness of the liquid layer at the cavity base is approximately 2% to 4% of the total penetration for those cases considered.

While the X-ray exposures supplied readily available information on penetration, the major value of these exposures is the portrayal of the penetration mechanism.

As the weld is initiated, the beam vaporizes the material in its path and thus begins the formation of the cavity. This boring action continues until an equilibrium is established. Once this equilibrium is established, a constant cavity height or penetration is produced. Regardless of the welding

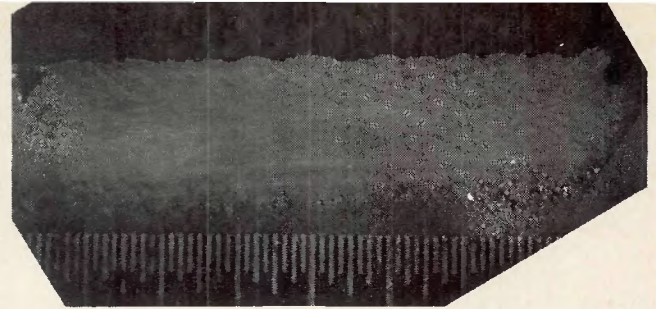


Fig. 4—Macrograph of sectioned weld No. 18; material: 6061 aluminum; welding conditions: $V = 150\text{KV}$, $i = 10\text{ ma}$; Etch: Kalling's reagent; Mag: 3.62X

speed, once the equilibrium cavity height is established, it remains at that height for the duration of the weld. One might expect that at zero welding speed that the beam would just continue its boring action. This has not been observed for welding times in place of up to 6 sec.

The time required to reach maximum or equilibrium penetration is less than 50 millisecc for all cases observed. Actual time depends on welding conditions and material, but in all cases it was less than 50 millisecc. Figure 5 illustrates a weld start. Since this time is so short, it can be concluded that welding speed has very little effect on the time to equilibrium.

Once the beam has reached full penetration, one might expect a rather static situation. If this were true, the X-ray exposures would just show the cavity base where the electrons are hitting. Observation of the exposures show that this is not the case. What is seen on the exposures are spots or regions along the cavity height where EB electrons are colliding with material (best illustrated in Figs. 5 and 6). These regions change location with time. At one time the beam may be striking on the cavity base. A few millisecc later the beam may be striking half way up the cavity or even very near the surface. Since the beam strikes at different locations in the cavity, material has come into the cavity to cut off the beam from the cavity base. The material must be liquid metal falling into the cavity from the surrounding cavity walls. These closures are evident from the X-ray exposures.

Figure 3 provides additional evidence for the closures since this macrograph of a weld cross-section shows several closures in the cavity. The material used for this weld is 6061 aluminum. Because of the high thermal conductivity of this material, rapid freezing can be expected when the electron beam is abruptly stopped. It is just by happenstance that the beam was terminated with the closures present. Rapid cooling of this material preserved this instant resulting in the capture of a closure.

One can suggest a reason for the

occurrence of these closures. As the beam strikes the cavity base, it rapidly heats the liquid at the base and pushes it up the cavity walls, most likely in a whirling fashion. The liquid metal is in dynamic motion but soon it becomes unstable as centrifugal force no longer holds it against the walls of the cavity. As the liquid layer begins to thicken, it ceases the upward movement and finally begins to fall back into the cavity. The coalescing to fall back is a closure.

Once the closure forms, it intersects the beam. Lower portions of the cavity are not being heated and are then given time to cool and even solidify. The closure is now accepting the EB energy. The closure, now superheated, falls back into the cavity.

Figure 8 illustrates this closure-fallback mechanism. While the closure-fallback mechanism is in operation, a dynamic equilibrium exists resulting in uniform penetration. Examination of the films shows that this pulsing may proceed for 50 to 150 cycles in a quite uniform way. However, there appears to be an occasional interruption of this closure-fallback mechanism in which the cavity is cleared of metal and the beam drills on the base of the cavity for an

extended period of time, producing a spike. It is believed that the closure becomes increasingly superheated as it pulsates in the cavity and finally is vaporized and possibly ionized to produce an "explosion" in which most of the closure droplet is expelled from

the hole. With the closure removed, the beam is now free to continue to the cavity base where a spike results.

The large spike seen in Fig. 7 illustrates the point. For some reason, a closure did not form and the beam has dwelled for an extended time at the

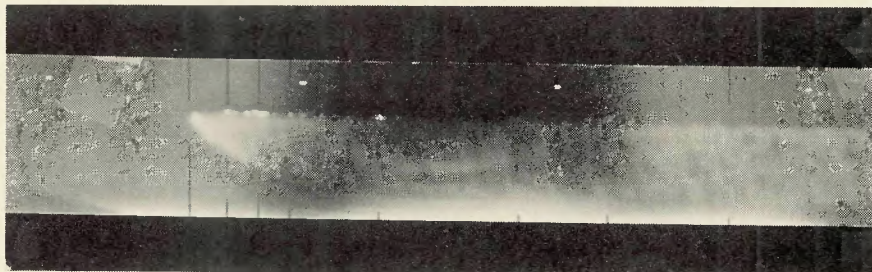


Fig. 5—Contact print of X-ray exposure for start of Run No. 41. Dots are present for timing purposes. Time between dots is 0.053 sec. Mag: 2.00X

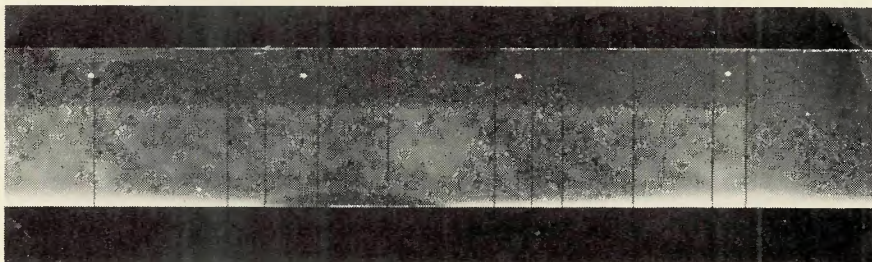


Fig. 6—Contact print of X-ray exposure for end of Run No. 41. Dots are present for timing purposes. Time between dots is 0.053 sec. Mag: 2.00X

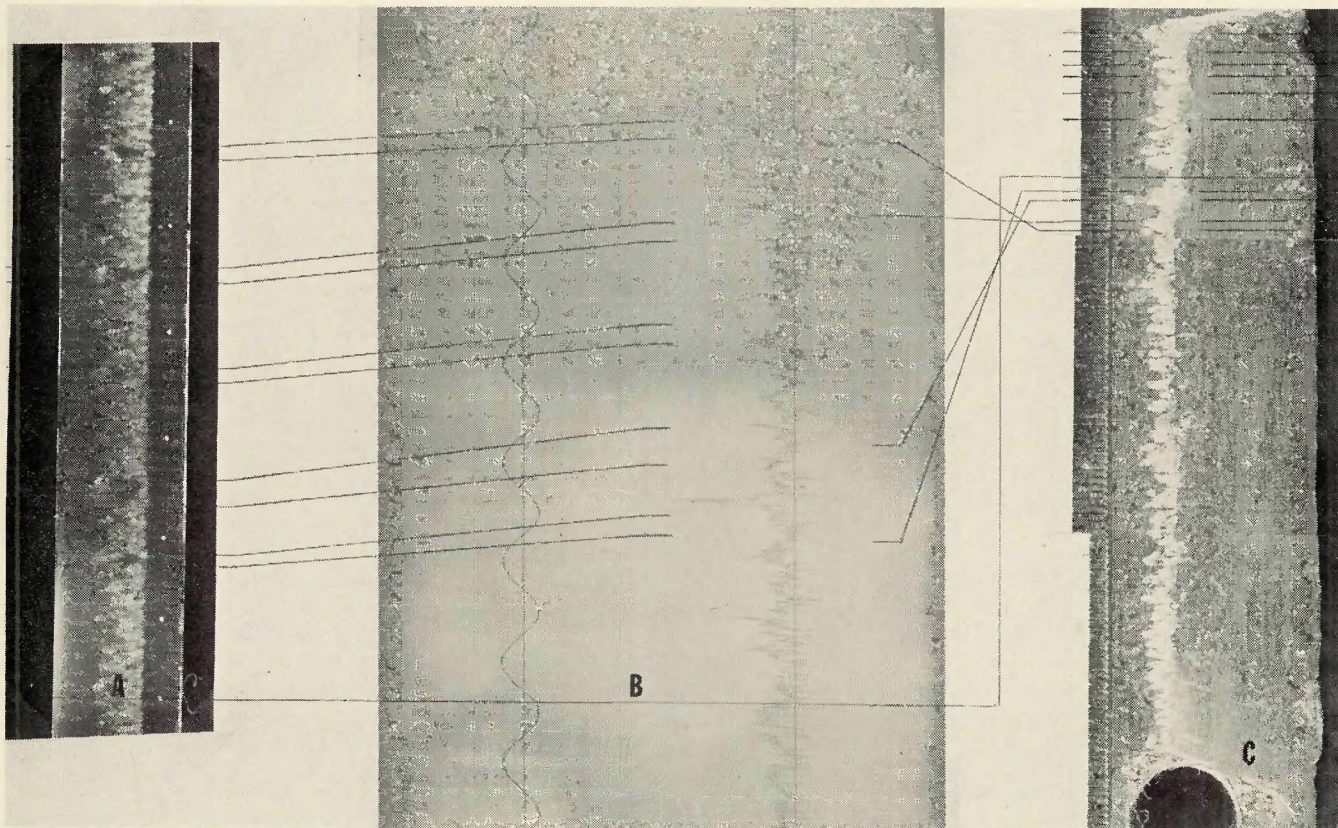


Fig. 7—Correlation of photomicrograph of cracked joint, grid voltage trace and contact print of X-ray exposure for middle of Run No. 40. Correlations are made by computing time for a given distance from known speeds. Reference lines correlate locations at equal times. A—Photomicrograph of cracked joint; material: 6061 aluminum; welding conditions: 150KV, 10 ma, 22.0 ipm; Mag: 5.00X. B—Oscillographic recording of grid voltage trace. Sine wave is used for timing purposes. It has a period of 0.053 sec. Voltage polarity-side toward X-ray print is negative. C—Contact print of X-ray exposure; dots present are for timing purposes. Time between dots is 0.053 sec. Mag 1.675X

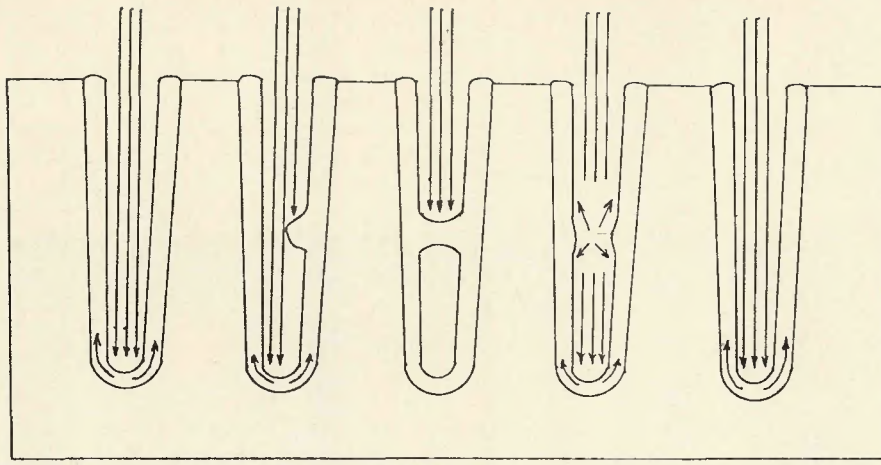


Fig. 8—Simulated closure/fall-back mechanism

cavity base. As a result, there is seen an increase in penetration at that region, or a spike.

It would seem that for most materials, spiking is indeed inherent. Break-downs of the closure-fallback mechanism occur to produce spikes. However, this does not rule out the possibility that the penetration mechanism cannot be appropriately controlled so as to eliminate spiking. Obviously, this would require a more sophisticated welding procedure such as interrupted cycles.

Although this mechanism can account for spiking, other defects might find their cause with this mechanism. For example, porosity in the fusion zone could result when a closure forms and does not fall back completely, but freezes off. A portion of the cavity would be trapped resulting in porosity. Or two closures might form simultaneously as the liquid boils up the cavity. If the beam is at this point long enough to explode only the upper closure, the lower closure could freeze in the lower part of the cavity to yield porosity.

It is well known that fusion zone of an EB weld is very homogeneous due to excellent metal mixing. The films show the turbulence in the cavity due to the pumping action of the beam and the formation of closures at various locations in the cavity that would mix the liquid quite thoroughly.

The grid detection system was installed to measure the voltage above the weld. If closures were being "exploded" by possible ionization, this grid might also detect this mechanism. Figure 7 gives a typical grid recording for a weld while being correlated in time with the X-ray exposure and the macrograph. What is suggested is that an electron coming from a closure is collected by this grid, producing a signal. However, the signal is not con-

clusive evidence of the mechanism since a multitude of other events can produce a voltage change in the grid. At any rate, while the experimental evidence is not conclusive, a correlation may exist between grid voltage spikes and closure explosions. Further experiments are planned to determine if a correlation does in fact exist.

Conclusions

From the evidence collected for partial penetration electron beam welding, the following conclusions are possible:

1. The pinhole camera technique can be used to observe the process or mechanism of electron beam penetration.
2. Extreme caution must be used when the method of grinding and polishing to the weld centerline is used in longitudinal sectioning to expose the maximum penetration of the weld. The resulting correlation with the penetration "seen" by the pinhole camera will be erroneous if caution is not exercised.
3. The method of cracking open butt joints made from butting together surface ground surfaces reliably exposes the maximum penetration. This reliability is essential for valid correlation of the actual penetration with the penetration "seen" by the pinhole camera.
4. The approximate thickness of the liquid layer at the cavity base is about 2 to 4% of the total penetration and is likely controlled by the thermal conductivity of the material.
5. From the X-ray exposures, the penetration mechanism of partial penetration electron beam welding is clarified. With initiation of the beam, the beam vaporizes the material as it bores its way into the material. Full penetration is reached within 50 millisecc with the establishment of an

equilibrium cavity. The beam, impinging on the cavity base, boils heated liquid up the walls of the cavity, most likely in a whirling fashion. Complete metal mixing results due to this dynamic pumping action. Cavity closures are produced as the metal loses kinetic energy. Once a closure forms, it intersects the electron beam producing two effects. First, while the beam is heating the closure, regions below the closure are given time to cool. Second, the closure is heated and generally falls back into the cavity and the cycle recurs. However, the closure may occasionally be vaporized in an explosion. After closure explosion, the cavity is clear of liquid and the beam is again free to impinge on the cavity base causing a spike. However, much more frequently the closure falls back into the cavity. This cyclic mechanism continues (at a typical rate of 150 cycles per sec) as an equilibrium process.

6. Spiking results when there is a failure or interruption of the cyclical closure-fallback mechanism. When a closure fails to materialize or is exploded out, the electron beam is free to dwell on the cavity base for a longer time, thus producing a penetration spike.

7. The technique of monitoring the charge above the weld with a voltage grid, although not conclusive, may be useful. The grid records the activity in the cavity, but the magnitude of voltage spikes is apparently a function of the location of the closure explosion with respect to the cavity opening and not necessarily related to closure explosion magnitude.

Acknowledgments

This work was conducted from funding provided by the Atomic Energy Commission from Union Carbide Corporation, Oak Ridge, Tennessee, under Contract W-7405-3ng-25, Subcontract 3347. In particular, Paul Turner is recognized for his support and interest in this work.

Also, appreciation is extended to the Department of Welding Engineering of The Ohio State University for the support and equipment made available.

References

1. Matsuda, Fukuhisa, and Hashimoto, Tatsuya, "Compilation of the Reports Published on 'Studies on Electron-Beam Welding'" (a compilation of nine articles appearing in *Transactions of National Research Institute for Metals*), April, 1970.
2. Tong, Henry, *Heat Transfer and Cavity Penetration During Electron Beam Welding*, Report No. 69-14 for work sponsored by Lawrence Radiation Laboratory, Livermore, California, June 1, 1969.

New Welding Research Council Bulletin Available

WRC
Bulletin
No. 166
October 1971

"Derivation of Code Formulas for Part B Flanges"

By E. O. Waters

New rules for bolted flanged connections appeared in the 1968 and 1970 Winter Addenda of the ASME Boiler and Pressure Vessel Code, and more recently in the 1971 edition of Section VIII, Division 1, providing for flanges with metal-to-metal contact outside the bolt circle. The development of this material came from recent work of the PVRC Design Division subcommittee that was assigned this topic.

There is considerable novelty in the formulas and charts in these rules, and it was the belief of the subcommittee members that their acceptance and understanding by Code users would be greatly aided if a concise account of their derivation were given. The paper was written with this in mind, and with the added purpose of providing a source to which reference could be made in the future, when specific inquiries have to be answered or revisions are contemplated.

Publication of this paper was sponsored by the Pressure Vessel Research Committee of the Welding Research Council. The price of Bulletin 166 is \$3.50 per copy. Orders for single copies should be sent to the American Welding Society, 2501 N.W. 7th St., Miami, Fla. 33125. Orders for bulk lots, 10 or more copies, should be sent to the Welding Research Council, 345 East 47th Street, New York, N. Y. 10017.

New Welding Research Council Bulletin Available

WRC
Bulletin
No. 167
November 1971

"Laser Welding and Cutting"

by M. M. Schwartz

The advent of high intensity low momentum surface heating devices is having a natural impact on the field of materials processing, particularly fusion welding. The laser and electron beam offer potential capability for precise control of energy and location which cannot be approached by older sources such as arcs and flames, and the fact that under certain operating conditions they transmit little or no thrust to the material being worked is an important advantage. However, the extreme intensity of these sources, expressed in dimensions of power per unit area, presents problems as well as advantages when addressed to the objective of local melting as in fusion welding.

The newest and most exciting of the two aforementioned processes is the "laser" (sometimes called optical maser). The laser represents a virtually brand-new scientific development. The possibility of a laser was first suggested in 1958 and the first experimental model was made in 1960. Since that time, advances in laser technology have been rapid and dozens of laboratories are performing laser research. Although much of this research is of a basic scientific nature many of the newer developments can be applied to welding. Experimental laser machines are already in use. No basic scientific discovery in history has been applied so fast to metalworking.

This report, prepared for the Interpretive Reports Committee of the Welding Research Council, reviews the basic principles of the laser and describes techniques, problems, advantages and disadvantages of using the laser for welding and cutting various materials.

The price of Bulletin 167 is \$3.50 per copy. Orders for single copies should be sent to the American Welding Society, 2501 N.W. 7th St., Miami, Fla. 33125. Orders for bulk lots, 10 or more copies, should be sent to the Welding Research Council, 345 East 47th Street, New York, N. Y. 10017.